

Ab initio Based Configuration Interaction Study of the Electronic Spectrum of GeS

Antara Dutta, Surya Chattopadhyaya, and Kalyan Kumar Das*

Department of Chemistry, Physical Chemistry Section, Jadavpur University, Calcutta 700 032, India

Received: July 25, 2000; In Final Form: December 18, 2000

The electronic spectrum of GeS has been studied by using ab initio based multireference configuration interaction calculations which include relativistic effective core potentials of Ge and S atoms. Potential-energy curves of 27 Λ -S states of GeS correlating with two dissociation limits have been computed. Spectroscopic constants of bound states are computed and compared with some of the observed states such as $X^1\Sigma^+$, $a^3\Sigma^+$, $b^3\Pi$, $A^1\Pi$, and $E^1\Sigma^+$. The ground state of GeS is composed of two dominant configurations: $...s^2\pi^4$ and $...s^2\pi^3\pi^*$ with $r_e = 2.039$ Å and $\omega_e = 549$ cm⁻¹, which compare well with the observed values. The ground-state dissociation energy of GeS is also estimated. The observed E state is assigned to $2^1\Sigma^+$. Effects of the spin-orbit coupling have been explored on 18 Λ -S states all of which converge with the lowest dissociation limit $^3P_g(\text{Ge}) + ^3P_g(\text{S})$. Potential-energy curves of all 50 Ω states arising from the spin-orbit interactions in these Λ -S states are computed. Transition probabilities of some dipole-allowed transitions are estimated. Transitions such as $b^3\Pi_{0+} - X^1\Sigma_{0+}^+$ and $b^3\Pi_1 - X^1\Sigma_{0+}^+$ which are analogous to the Cameron bands of the isovalent CO are investigated. The observed $a^3\Sigma_1^+ - X^1\Sigma_{0+}^+$ transition of GeS is also studied. Radiative lifetimes of $A^1\Pi_1$, $E^1\Sigma_{0+}^+$, $a^3\Sigma_1^+$, $b^3\Pi_{0+}$, $b^3\Pi_1$, and some other components are estimated.

I. Introduction

Experimental studies of molecules and clusters of group IV–VI atoms have been the subject of research for the past several decades.^{1–30} In recent years,^{5–9} there are many spectroscopic investigations on the diatomics of silicon such as SiX (X = O, S, Se, and Te). These are mainly concerned with the E–X bands in the ultraviolet and visible regions. The bands in the visible region are observed only in the emission. On the other hand, there are less amount of data available for the analogous germanium compounds. The molecules formed by germanium and group VIB atoms are known to be good semiconductors as well. At low temperature, superconductivity has been observed for GeTe, though it is a semiconductor molecule. Barrow and co-workers^{1–3} have studied ultraviolet absorption spectroscopy of a series of diatomic molecules such as GeO, GeS, GeSe, and GeTe. These molecules have shown strong D–X bands in the UV region. Some weak bands of the type E–X have also been detected. The vibrational analyses of the D–X system of GeSe and GeTe have been carried out from the measurements of the spectra emitted by the high-current positive-column discharges.¹ The ground states of these molecules are assigned as $X^1\Sigma^+$. The measurements suggest that $\nu'(0,0)$ of this band for GeS is around 32 889.5 cm⁻¹. The D–X band systems of these molecules have been reassigned as $A^1\Pi - X^1\Sigma^+$. Theoretical or experimental data regarding the transition probability of the A–X transition and lifetime of the $A^1\Pi$ state of GeS are not available as yet. Shapiro et al.¹⁰ have found two band systems, namely, $A^1\Pi - X^1\Sigma^+$ and $E^1\Sigma^+ - X^1\Sigma^+$, in the region of 3358–2709 and 2782–2464 Å, respectively. These bands are vibrationally analyzed. However, the rotational analysis of these bands was difficult because of the overlapping bands of natural abundances of isotopomers of GeS.³ The rotational

spectra of GeS and GeSe have been measured in the frequency range of 66–110 GHz with high precision.¹¹ Magat et al.¹² have carried out the rotational analysis of a few bands belonging to the A–X system by using the available ground-state rotational constants.

Coppens et al.¹³ have determined the dissociation energies of the gaseous monosulfides such as GeS, ScS, YS, LaS, and CeS by using a mass spectrometer. The dissociation energy of the E state derived from the vibrational analysis³ is found to be 0.9 eV, and the dissociated product is Ge(³P) + S(³P). The ground states of these molecules converge with Ge(³P₀) + X(³P₂) (X = O, S, Se, and Te) limits. The dissociation energy of the ground state of GeS has been estimated to be 5.66 ± 0.13 eV. Marino et al.¹⁴ have studied infrared spectra of the matrix-isolated germanium, tin, and lead chalcogenides. Fundamental vibrational frequencies of these molecules have been reported in a vapor, argon, and N₂ matrix at low temperature. The hyperfine structure and dipole moments of the diatomic molecules of group IV–VI have been obtained from the Stark-effect measurement on the pure rotational transitions.^{15–18} A strong UV absorption corresponding to the lowest allowed transition $A^1\Pi - X^1\Sigma^+$ has been observed in the gas phase of GeO, GeS, SnO, and SnS.¹⁹ In the low-temperature matrix, only solvent-induced phosphorescence, which is assigned to the $a^3\Pi - X^1\Sigma^+$ transition, is observed. This transition resembles the Cameron bands of the isovalent CO. However, at that time, this transition had not been observed in the gas phase. The $a^3\Pi$ state is populated by the matrix-induced intersystem crossing from the $^1\Pi$ or $^1\Sigma$ states which are populated via an allowed absorption. Later on Linton²¹ had observed two new band systems in two different regions in a chemiluminescent flame produced by the reaction $\text{Ge} + \text{OCS} \rightarrow \text{GeS} + \text{CO}$. The previously known bands such as $A^1\Pi - X^1\Sigma^+$ and $E^1\Sigma^+ - X^1\Sigma^+$ are not present, whereas the new bands are assigned as $b^3\Pi_1 - X^1\Sigma^+$ and $a^3\Sigma^+ - X^1\Sigma^+$ in the regions 350–400 and 420–650

* To whom correspondence should be addressed. E-mail: kalyankd@hotmail.com

nm, respectively. It has been noted that these two excited states of GeS are analogous to the $a^3\Sigma^+$ and $a^3\Pi_r$ states of CO. The spectroscopic parameters of $a^3\Sigma^+$ and $b^3\Pi$ states are also reported in this experimental study.²¹ It has been suggested that the $b^3\Pi_1$ component of GeS would radiate to the ground state with significant intensity similar to GeO.²² In the matrix isolation studies at low temperature, Meyer and co-workers^{19,20} have observed phosphorescence from the low-lying state of GeS, which has been assigned as $a^3\Pi$. The assignment of this phosphorescence to $a^3\Pi-X^1\Sigma^+$ has been based on the expectation that the energy of the $^3\Pi$ state would be lower than that of $^3\Sigma^+$. However, further studies on SiO, GeO, and GeS show that the phosphorescence originates from the $a^3\Sigma^+$ state.²¹

More recently Balfour and Shetty²³ have observed a new group of bands in emission in the 500–600 nm region, in addition to the known A–X and E–X ultraviolet bands. They have concluded that these new bands constitute the long-wavelength component of the $E^1\Sigma^+-X^1\Sigma^+$ system of GeS. This has been confirmed from the vibrational analysis of the ultraviolet and visible bands. The infrared Fourier transform emission spectrum of GeS at 900 K has been observed by Uehara et al.²⁴ The vibration–rotational bands for different isotopomers have been assigned between 520 and 605 cm^{-1} . Hassanzadeh and Andrews²⁵ have recently prepared GeO, GeS, and their mixed XGeY (X, Y=O, S) compounds from the reactions of atomic germanium with oxygen and sulfur in argon matrices and characterized by the infrared absorption spectroscopy. The fundamental frequencies of these products have been assigned. These authors have established that the bonds in triatomic XGeX species are shorter than those in GeX molecules.

Theoretical calculations of these molecules are seldom attempted. Köppe and Schnöckel²⁶ have performed ab initio based Hartree–Fock (HF) calculations for the ground-state geometries of GeX, GeY, and XGeY (X, Y=O, S) molecules. Recently, Leszczyński and Kwiatkowski²⁷ have also studied these molecules along with their heavier counterparts such as GeSe, OGeSe, SGeSe, and SeGeSe at the HF and the second-order Møller–Plesset perturbation theory (MP2) level. The molecular parameters, dipole moments, and rotational constants of these molecules are predicted. Ogilvie²⁸ has estimated the electric dipolar moment and rotational g factor of GeS from the analysis of frequencies and wavenumbers of pure rotational and vibration–rotational spectra. In recent years, large scale ab initio based configuration interaction (CI) calculations on the ground and low-lying excited states of the isovalent molecules such as GeSe and GeTe have been performed.^{29,30} Using the available relativistic effective core potentials (RECPs) and spin–orbit operators, one can investigate the spectroscopic features of these molecules more accurately.

In this paper, we report computations of potential-energy curves and spectroscopic features of low-lying electronic states of GeS by using ab initio based multireference singles and doubles configuration interaction (MRDCI) method, including the relativistic effects through effective core potentials. Spin–orbit interaction has been taken into consideration extensively. Transition probabilities of several dipole-allowed transitions are discussed. Of these, transitions such as $A^1\Pi_1-X^1\Sigma_0^+$, $E^1\Sigma_0^+-X^1\Sigma_0^+$, $a^3\Sigma_1^+-X^1\Sigma_0^+$, $b^3\Pi_0^+-X^1\Sigma_0^+$, and $b^3\Pi_1-X^1\Sigma_0^+$ are of special interest with reference to their experimental findings. The computed radiative lifetimes of some excited states such as $A^1\Pi_1$, $a^3\Sigma_1^+$, $b^3\Pi_0^+$, and $b^3\Pi_1$ are reported in a separate subsection.

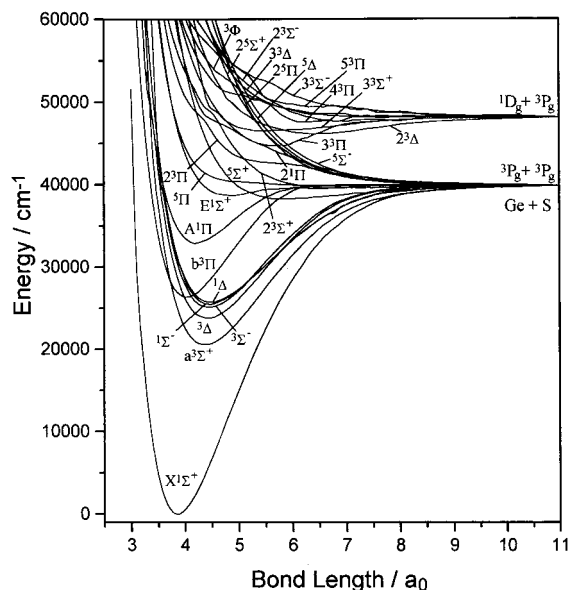
II. Computational Details

The computations have been carried out by using semi-core RECPs of Ge and S as reported by Hurley et al.³¹ and Pacios and Christiansen.³² The $3d^{10}4s^24p^2$ electrons of Ge and $3s^23p^4$ electrons of S have been kept in the valence space, whereas the remaining electrons are substituted with the semi-core RECPs. This will reduce the total number of active electrons for GeS to 20. The primitive Gaussian basis sets which are compatible with the RECPs are used in the present calculations. For the germanium atom, the basis sets of the type (3s3p4d) are taken from Hurley et al.³¹ The (4s4p) Gaussian basis sets³² of the sulfur atom are augmented with a set of d functions of an exponent 0.65, so that the final basis set is of the type (4s4p1d). To carry out CI calculations, one needs a set of optimized symmetry-adapted self-consistent-field molecular orbitals (SCF-MOs) as one-electron basis functions. For GeS, we have performed SCF calculations for the $... \pi^3 \pi^* \Delta$ state with 20 valence electrons at different internuclear distances of the potential-energy curves. Conventionally, we have placed the molecule along the Z -axis, and the entire calculations have been carried out in the C_{2v} subgroup of the actual $C_{\infty v}$ point group in which the molecule belongs. Although $3d^{10}$ electrons are kept in the valence space, the preliminary analyses of the symmetry-adapted SCF-MOs at any bond length show that these d electrons more or less remain localized on the d orbitals of the Ge atom. These $3d^{10}$ electrons of the Ge atom do not participate much in the formation of the Ge–S bond in the low-lying excited states of the molecule. These electrons are, therefore, not allowed to excite in the CI steps. The MRDCI methods of Buenker and co-workers^{33–37} have been employed throughout the calculations. The table-CI algorithm^{33–37} has been used for the open-shell configurations. In this method, a set of main reference configurations are chosen for low-lying excited states of a given spin and spatial symmetry. For each Λ -S symmetry, eight lowest roots are calculated. Single and double excitations from these reference sets are being carried out. These excitations generate a large number of configurations for a particular symmetry. A configuration-selection technique has been employed to reduce the size of the secular equation. In addition, the energy-extrapolation method along with the Davidson's corrections^{38,39} gives an estimate of the full-CI energies in the same atomic orbital basis. The threshold chosen for the configuration-selection technique is $1 \mu\text{hartree}$ throughout the calculations. The largest selected CI space has the dimension of 36 000. Singlet, triplet, and quintet states up to 40 000 cm^{-1} of energy have been investigated. In the present calculations, the sum of the squares of coefficients of the reference configurations for each root is always above 0.90. The CI energies and wave functions are used for the calculations of spectroscopic constants, potential-energy curves, and one-electron properties of the GeS molecule.

The spin–orbit operators which are compatible with the RECPs of Ge and S are taken from Hurley et al.³¹ and Pacios and Christiansen,³² respectively. The spin-independent CI wave functions are multiplied with appropriate spin functions, which transform as C_{2v} irreducible representation. The diagonals of the spin-included Hamiltonian matrix consist of full CI energies of the Λ -S CI calculations. The off-diagonal elements are computed by the RECP-based spin–orbit operators and Λ -S CI wave functions. In the C_{2v} group, A_1 , A_2 , and B_1 representations consist of all spin–orbit states in the calculations. The secular equations are, therefore, blocked into three sets. In the present calculations, the sizes of the secular equations corresponding to A_1 , A_2 and B_1 blocks are 46×46 , 45×45 , and

TABLE 1: Dissociation Correlation between the Molecular and Atomic States of GeS in the Absence of Spin–Orbit Interaction

Λ -S states	atomic states Ge + S	relative energy, cm^{-1}	
		expt ^a	calcd
$^1\Sigma^+(2), ^1\Sigma^-, ^1\Pi(2), ^1\Delta,$ $^3\Sigma^+(2), ^3\Sigma^-, ^3\Pi(2), ^3\Delta,$ $^5\Sigma^+(2), ^5\Sigma^-, ^5\Pi(2), ^5\Delta$	$^3P_g + ^3P_g$	0	0
$^3\Sigma^+, ^3\Sigma^-(2), ^3\Pi(3), ^3\Delta(2), ^3\Phi$	$^1D_g + ^3P_g$	7125	8269

^a Reference 41.**Figure 1.** Potential-energy curves of Λ -S states of GeS.

46 \times 46, respectively, on the basis of the number of roots in the Λ -S treatment. Therefore, the inclusion of the spin–orbit interactions is done in a two-step variational method. The spin–orbit CI wave functions are finally analyzed in terms of Λ -S eigenfunctions. Spectroscopic features of spin–orbit states are obtained by fitting potential-energy curves of bound states and solving the vibrational Schrödinger equations numerically.⁴⁰ The vibrational energies and wave functions are used for computing electronic transition moments for the pair of vibrational functions involved in a particular transition. Einstein spontaneous emission coefficients and hence transition probabilities are calculated subsequently. Finally, the radiative lifetimes of the excited states at different vibrational levels are estimated from transition probability data.

III. Discussion of the Computed Results

Low-lying Λ -S states. The ground states of both Ge and S atoms belong to the 3P_g symmetry. Eighteen Λ -S states of singlet, triplet, and quintet spin multiplicities correlate with the lowest dissociation limit $\text{Ge}(4s^24p^2; ^3P_g) + \text{S}(3s^23p^4; ^3P_g)$. As seen from Table 1, the interaction between $\text{Ge}(^1D_g)$ and $\text{S}(^3P_g)$ states produces nine Λ -S triplet states of the GeS molecule. The experimental relative energies⁴¹ which are averaged over j are shown in Table 1. The calculated energy of the $\text{Ge}(^1D_g) + \text{S}(^3P_g)$ limit with respect to the lowest one is found to be 8269 cm^{-1} as compared with the observed value of 7125 cm^{-1} . In the present study, we have mainly focused our attention on those states which converge with the lowest two dissociation limits. Figure 1 shows the potential-energy curves of all 27 Λ -S states correlating with the lowest two asymptotes. Spectroscopic

TABLE 2: Spectroscopic Constants of Λ -S States of GeS

state	T_e, cm^{-1}	$r_e, \text{\AA}$	ω_e, cm^{-1}
$X^1\Sigma^+$	0	2.039 (2.012) ^a (2.028) ^b	549 (576) ^a (578) ^b (573.7; 577.6) ^d 359 (388.9 \pm 1) ^d
$a^3\Sigma^+$	20 521 (22 500 \pm 200) ^c (21 986.3 \pm 2.3) ^d	2.316	
$^3\Delta$	23 732	2.341	346
$^3\Sigma^-$	25 076	2.358	334
$^1\Sigma^-$	25 487	2.372	326
$^1\Delta$	25 702	2.379	315
$b^3\Pi$	26 357 (27 192 \pm 1.8) ^d	2.133	423 (435.4 \pm 1.1) ^d
$A^1\Pi$	32 960 (32 890) ^a	2.233	341 (375) ^a
$E^1\Sigma^+$	38 743 (38 885) ^a	2.582	184 (310) ^a

^a Reference 18. ^b Reference 27. ^c Reference 19. ^d Reference 21.

properties (r_e , ω_e , and T_e) of nine Λ -S bound states which are lying within 5 eV of energy are reported in Table 2. The ground-state symmetry of the GeS molecule is $X^1\Sigma^+$ as expected. The computed r_e and ω_e of the ground state are 2.039 \AA and 549 cm^{-1} , respectively. The values obtained from the vibrational and rotational analyses of the observed spectra¹⁸ are 2.012 \AA and 575.8 cm^{-1} , respectively. The vibrational frequencies of the $X^1\Sigma^+$ state as calculated from the observed $a^3\Sigma^+ - X^1\Sigma^+$ and $b^3\Pi - X^1\Sigma^+$ systems by Linton²¹ are 573.7 and 577.6 cm^{-1} , respectively. The ground-state r_e and ω_e of GeS, computed at the MP2 level by Leszczyński and Kwiatkowski,²⁷ are 2.028 \AA and 578 cm^{-1} , respectively. The discrepancies with our computed values are well within the accuracy of the MRDCI method under the effective core potential approximation. Although the ground state is the lowest $^1\Sigma^+$, it is not characterized by a pure closed-shell configuration. The calculations reveal that at r_e the ground state comprises two equally dominating configurations $\dots\sigma^2\pi^4$ ($c^2 = 0.67$) and $\dots\sigma^2\pi^3\pi^*$ ($c^2 = 0.22$). The first excited state of the $^3\Sigma^+$ symmetry is lying 20 521 cm^{-1} above the ground state. The MRDCI-estimated r_e and ω_e of this state are 2.316 \AA and 359 cm^{-1} , respectively. The $^3\Sigma^+$ state has been observed by Linton²¹ at 21 986.3 \pm 2.3 cm^{-1} , with $\omega_e = 388.9 \pm 1.0 \text{ cm}^{-1}$. Accordingly, we designate this state as $a^3\Sigma^+$ which is analogous to the $a^3\Sigma^+$ state of CO. The computed T_e and ω_e values are somewhat smaller than the observed values. The composition of the CI wave functions shows that the $a^3\Sigma^+$ state is predominantly $\dots\sigma^2\pi^3\pi^*$ ($c^2 = 0.82$). The Ge–S bond in $a^3\Sigma^+$ is weaker than the ground-state bond. The single excitation $\dots\pi^4 \rightarrow \dots\pi^3\pi^*$, which is responsible for the existence of the $a^3\Sigma^+$ state, also generates two triplets, namely, $^3\Sigma^-$ and $^3\Delta$, and three singlets, such as $^1\Sigma^+$, $^1\Sigma^-$, and $^1\Delta$. The ground-state itself has a 22% contribution of $\dots\sigma^2\pi^3\pi^*$, and there exists no other $^1\Sigma^+$ state which can be purely described by this configuration. Four other states, such as $^1,^3\Delta$ and $^1,^3\Sigma^-$, originate mainly from the $\dots\pi^4 \rightarrow \dots\pi^3\pi^*$ excitation. However, another open-shell configuration $\dots\sigma\sigma^*\pi^3\pi^*$ contributes to a smaller extent for these closely spaced Λ -S states. One may note that $^3\Sigma^-$, $^1\Sigma^-$, and $^1\Delta$ states are nearly degenerate, with transition energies lying in the range of 25 000–26 000 cm^{-1} . The Ge–S bonds in these states are somewhat longer than the ground-state bond. Their vibrational frequencies are found to be around 340 cm^{-1} , which is much smaller than the ground-state ω_e . None of these Λ -S states undergo symmetry-allowed transitions to the ground state. However, in the presence of the spin–orbit coupling, some transitions are allowed.

The $^3\Pi$ state of GeS is strongly bound, with $r_e = 2.133 \text{ \AA}$ and $\omega_e = 423 \text{ cm}^{-1}$. The state is lying $26\,357 \text{ cm}^{-1}$ above the ground state, and at r_e , it is predominantly composed of $...\sigma\pi^4\pi^*$ ($c^2 = 0.75$) and $...\sigma\pi^3\pi^{*2}$ ($c^2 = 0.12$) configurations. The characteristics of the SCF-MOs show that σ is a strongly bonding MO consisting of s and p_z atomic orbitals of Ge and S. The second π MO is antibonding involving p_{xy} atomic orbitals of the constituent atoms. Therefore, $\sigma \rightarrow \pi^*$ excitation in the $^3\Pi$ state makes the Ge–S bond slightly weaker as compared with the ground-state bond. Although the transition from $^3\Pi$ to the ground state is forbidden, the spin–orbit components ($\Omega = 0^+$ and 1) of $^3\Pi$ would undergo allowed transitions. Some important results are obtained from the extrapolation of the observed phosphorescence spectra^{19,20} in various solid matrixes at low temperature. Meyer et al.^{19,20} have assigned the phosphorescence spectrum of GeS to $a^3\Pi-X^1\Sigma^+$ with the expectation that the $^3\Pi$ state would be lower than $^3\Sigma^+$. However, more recent work²¹ concludes that the phosphorescence takes place from the $a^3\Sigma^+$ state, which is lower than $^3\Pi$. The value of T_{00} of $a^3\Sigma^+$ obtained from the phosphorescence data has been estimated as $22\,500 \pm 200 \text{ cm}^{-1}$, and the gas-phase value²¹ has been calculated as $21\,894 \text{ cm}^{-1}$. Our calculations confirm Linton's²¹ conclusion that the $^3\Sigma^+$ state is lower than that of $^3\Pi$ by about 5000 cm^{-1} . Accordingly, we have designated the $^3\Pi$ state as $b^3\Pi$. It has been predicted that the $b^3\Pi_1$ component should radiate to the ground state with significant intensity. Capelle and Brom²² have explained a similar effect for GeO on the basis of large spin–orbit coupling in the $^3\Pi$ state. The calculated T_e and ω_e values of $b^3\Pi$ are in good agreement with the observed values of $27\,192 \pm 1.8$ and $435.4 \pm 1.1 \text{ cm}^{-1}$, respectively. Transition probabilities of both spin-forbidden transitions such as $a^3\Sigma^+-X^1\Sigma^+$ and $b^3\Pi-X^1\Sigma^+$ are the prime objectives in the present work. The $b^3\Pi-X^1\Sigma^+$ transition corresponds to the spin-forbidden Cameron bands of the isovalent CO. The present calculations show that there are two states, namely, $^3\Sigma^+$ and $^3\Delta$, between $20\,000$ and $24\,000 \text{ cm}^{-1}$ of energy. The $\Omega = 1$ components of both $^3\Sigma^+$ and $^3\Delta$ may also radiate to the ground-state component.

The singlet counterpart of $^3\Pi$ is also generated from the same single excitation $\sigma \rightarrow \pi^*$. The $^1\Pi$ state is designated as the A state in accordance with the observed $A^1\Pi \leftrightarrow X^1\Sigma^+$ transition.^{2,3,10} The calculated transition energy of $A^1\Pi$ is $32\,960 \text{ cm}^{-1}$, which is in excellent agreement with the observed A–X band around $32\,890 \text{ cm}^{-1}$. The D–X band system as mentioned by Barrow and co-workers^{1–3} corresponds to same A–X transition. The MRDCI-estimated r_e and ω_e values of the $A^1\Pi$ state are 2.233 \AA and 341 cm^{-1} , respectively. Although the experimental r_e of the $A^1\Pi$ state is not yet known, the observed ω_e value is about 34 cm^{-1} larger than the calculated one (see Table 2). Such an underestimation of the vibrational frequencies is consistent throughout the calculation.

The excited $^1\Sigma^+$ state, which has been denoted as E, is weakly bound. The shallow potential well contains only 4–5 vibrational levels. The computed transition energy of the $E^1\Sigma^+$ state is $38\,743 \text{ cm}^{-1}$, whereas r_e and ω_e are 2.582 \AA and 184 cm^{-1} , respectively. The calculated ω_e is, however, considerably small compared with the experimental value of 310 cm^{-1} as derived from the UV absorption spectra of the E–X band system of the molecule.¹¹ The E state is assigned to the $^1\Sigma^+$ symmetry.^{3,10} The $E^1\Sigma^+-X^1\Sigma^+$ band has been vibrationally analyzed. The present calculations reveal that there are no other bound states around $38\,000 \text{ cm}^{-1}$ except $2^1\Sigma^+$. The next available bound state ($3^1\Sigma^+$) lies above $48\,000 \text{ cm}^{-1}$. The compositions of the CI wave functions show that the $E^1\Sigma^+$ state is dominated by the $...\pi^2\pi^{*2}$

TABLE 3: Dissociation Relation between Ω States and Atomic States of GeS with Spin–Orbit Coupling

Ω state	atomic states Ge + S	relative energy, $\text{cm}^{-1} \text{ expt}^a$
$0^+, 1, 2$	$^3P_0 + ^3P_2$	0
$0^-, 1$	$^3P_0 + ^3P_1$	397
$0^+, 0^-(2), 1(3), 2(2), 3$	$^3P_1 + ^3P_2$	557
0^+	$^3P_0 + ^3P_0$	574
$0^+(2), 0^-, 1(2), 2$	$^3P_1 + ^3P_1$	954
$0^-, 1$	$^3P_1 + ^3P_0$	1131
$0^+(3), 0^-(2), 1(4), 2(3), 3(2), 4$	$^3P_2 + ^3P_2$	1410
$0^+, 0^-(2), 1(3), 2(2), 3$	$^3P_2 + ^3P_1$	1807
$0^+, 1, 2$	$^3P_2 + ^3P_0$	1984

^a Reference 41.

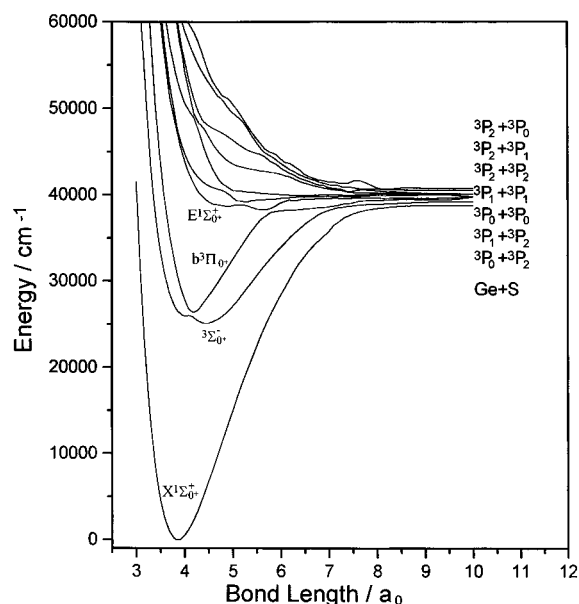
configuration. Several other configurations contribute significantly to the $E^1\Sigma^+$ state. The closed-shell configuration $...\pi^4$ has a 26% contribution to the composition of the $E^1\Sigma^+$ state. Excited triplets such as $2^3\Pi$, $3^3\Pi$, $^3\Delta$ etc. are mostly repulsive in nature. All six quintet states such as $^5\Sigma^+$, $2^5\Sigma^+$, $^5\Sigma^-$, $^5\Pi$, $2^5\Pi$, and $^5\Delta$ correlating with the $^3P_g + ^3P_g$ limit are repulsive.

Mass spectrometric study¹³ has determined the ground-state dissociation energy of GeS as $5.66 \pm 0.13 \text{ eV}$ using thermochemical data. The present MRDCI calculations predict the value as 4.95 eV , which is somewhat smaller than the experimentally derived value. The underestimation of the dissociation energy has been noted in all previous calculations using the present methodology. In similar calculations on GeSe and GeTe the computed D_e values are about 0.3 – 0.4 eV smaller than the observed data.^{29,30} A part of the discrepancy is due to the RECP approximation. However, some improvement is also expected if $3d^{10}$ electrons of Ge are correlated in the CI step. There remains a scope for the enhancement of basis sets. The dissociation energy of the $A^1\Pi$ state is computed to be 0.88 eV , whereas that of the $E^1\Sigma^+$ state is only 0.16 eV .

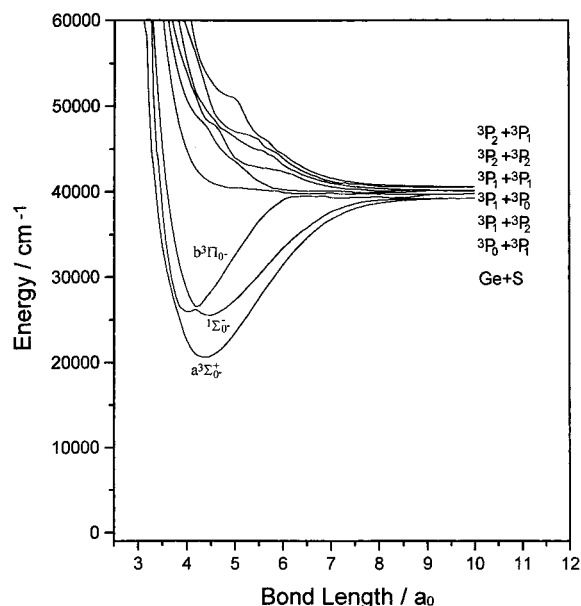
Effects of the Spin–Orbit Interaction. In this section, we discuss the effects of the spin–orbit coupling introduced in the above-mentioned Λ -S states of the molecule. For this purpose we are confined with all possible Ω states which are obtained from 18 Λ -S states converging with the lowest $\text{Ge}(^3P_g) + \text{S}(^3P_g)$ limit. Table 3 shows all 50 Ω states of 0^+ , 0^- , 1, 2, 3, and 4 symmetries which split into nine asymptotes. The observed relative energies of these dissociation limits are also given in Table 3. The present calculations show that only 16 spin–orbit states are bound within $40\,000 \text{ cm}^{-1}$ of energy. The ground state is not perturbed by the spin–orbit coupling because there are no nearby 0^+ components for interactions. Spectroscopic constants of this component remain unchanged as shown in Table 4. There are 10 0^+ components correlating with seven dissociation limits. The computed potential-energy curves of these components are shown in Figure 2. Only four spin–orbit components with $\Omega = 0^+$ have bound characters, and others are repulsive. In Figures 3–5, we have shown potential-energy curves of the remaining components with $\Omega = 0^-, 1, 2, 3,$ and 4 . There are at least six Λ -S states whose transition energies are very close to each other. So, potential-energy curves of the components with same Ω undergo avoided crossings in the Franck–Condon region. The spin–orbit interactions for the light molecules like GeS are comparatively small. In general, the diabatic curves are fitted for estimating spectroscopic parameters. Table 4 shows that all of the spin–orbit components are composed of almost pure Λ -S states in the Franck–Condon region. We have also tabulated the composition at larger distances, (say, $6.0 a_0$) to show the extent of spin–orbit interactions. Two spin–orbit components of $a^3\Sigma^+$ are separated

TABLE 4: Spectroscopic Constants of Ω States of GeS with the Spin–Orbit Coupling

state	T_e , cm^{-1}	r_e , \AA	ω_e , cm^{-1}	composition	
				at r_e	at $6.0 a_0$
$X^1\Sigma_0^+$	0	2.041	548	$X^1\Sigma^+(99)$	$X^1\Sigma^+(99)$
$a^3\Sigma_1^+$	20 373	2.326	357	$a^3\Sigma^+(98), ^3\Sigma^-(2)$	$a^3\Sigma^+(95), ^3\Sigma^-(5)$
$a^3\Sigma_0^+$	20 470	2.321	359	$a^3\Sigma^+(99)$	$a^3\Sigma^+(99), ^1\Sigma^-(1)$
$^3\Delta_2$	23 357	2.341	344	$^3\Delta(92), ^1\Delta(8)$	$^3\Delta(45), ^1\Delta(55)$
$^3\Delta_1$	23 429	2.342	346	$^3\Delta(99)$	$^3\Delta(99)$
$^3\Delta_3$	23 894	2.341	347	$^3\Delta(99)$	$^3\Delta(99)$
$^3\Sigma_{0+}^-$	25 069	2.361	336	$^3\Sigma^-(99)$	$^3\Sigma^-(99)$
$^3\Sigma_1^-$	25 168	2.364	334	$^3\Sigma^-(98), a^3\Sigma^+(2)$	$^3\Sigma^-(94), a^3\Sigma^+(5)$
$^1\Sigma_0^-$	25 481	2.374	322	$^1\Sigma^-(99)$	$^1\Sigma^-(99), a^3\Sigma^+(1)$
$^1\Delta_2$	25 939	2.376	319	$^1\Delta(91), ^3\Delta(8)$	$^1\Delta(45), ^3\Delta(55)$
$b^3\Pi_{0-}$	25 923	2.139	422	$b^3\Pi(99)$	$b^3\Pi(94), 2^3\Sigma^+(5)$
$b^3\Pi_{0+}$	25 931	2.137	427	$b^3\Pi(99)$	$b^3\Pi(96), E^1\Sigma^+(2)$
$b^3\Pi_1$	26 261	2.137	429	$b^3\Pi(99)$	$b^3\Pi(78), 2^1\Pi(18), 2^3\Sigma^+(2)$ $^5\Pi(1)$
$b^3\Pi_2$	26 725	2.139	422	$b^3\Pi(99)$	$b^3\Pi(93), ^5\Pi(5)$
$A^1\Pi_1$	33 011	2.232	344	$A^1\Pi(99)$	$A^1\Pi(65), 2^5\Pi(16), 2^3\Pi(10)$ $2^5\Sigma^+(4), 2^3\Delta(2), 3^3\Pi(1)$
$E^1\Sigma_0^+$	38 745	2.562	190	$E^1\Sigma^+(99)$	$E^1\Sigma^+(96)$

**Figure 2.** Potential-energy curves of low-lying 0^+ states of GeS.

only by 100 cm^{-1} . The $\Omega = 1$ component is lying lower than the 0^- component. Other spectroscopic constants of these two components are very similar. The $a^3\Sigma_1^+$ component is important from the experimental point of view because the $a^3\Sigma_1^+ - X^1\Sigma_0^+$ band system has been observed.²¹ Of the three components of $^3\Delta$, the $\Omega = 3$ component is shifted upward, whereas the other two components ($\Omega = 1$ and 2) are shifted downward. The $^3\Delta_2$ component is found to be somewhat lower in energy, and at r_e , it is mixed with 8% of the $^1\Delta$ component. The spin–orbit splitting between the two components of $^3\Sigma^-$ is also very small. Figures 2 and 4 show that both $^3\Sigma_{0+}^-$ and $^3\Sigma_1^-$ components undergo sharp avoided crossings with the corresponding components of the $^3\Pi$ state. The components such as $^1\Sigma_0^-$ and $^1\Delta_2$ do not change much because of the spin–orbit coupling. Four components of $b^3\Pi$ split in the increasing energetic order such as $0^-, 0^+, 1,$ and 2 . The largest splitting was calculated to be about 800 cm^{-1} . Many sharp avoided crossings are noted in the potential-energy curves of these components. In each curve, the diabatic potential well is considered for estimating the spectroscopic constants. As seen from Table 4, the spin–orbit

**Figure 3.** Potential-energy curves of low-lying 0^- states of GeS.

effects on these components are not significantly large. However, $b^3\Pi_{0+}$ and $b^3\Pi_1$ components undergo allowed transitions to the ground-state component $X^1\Sigma_0^+$. The $b^3\Pi_1 - X^1\Sigma_0^+$ band has been experimentally observed in the ultraviolet region. The $A^1\Pi_1$ component lies $33\,011 \text{ cm}^{-1}$ above the ground-state. There is almost no mixing with other components of the same symmetry in the Franck–Condon region of the $A^1\Pi_1$ component. The $E^1\Sigma_0^+$ component remains as pure $E^1\Sigma^+$ with a shallow potential well consisting of only four vibrational levels.

Transition Properties and Radiative Lifetimes of the Excited States. In the absence of any spin–orbit interaction, $A^1\Pi$ and $E^1\Sigma^+$ are the only two states which undergo symmetry-allowed transitions such as $A^1\Pi - X^1\Sigma^+$ and $E^1\Sigma^+ - X^1\Sigma^+$. We have computed transition moments of these two transitions from MRDCI energies and wave functions. The transition moments of these two transitions as a function of the bond length are shown in Figure 6a. The transition moments of the $E^1\Sigma^+ - X^1\Sigma^+$ transition are comparatively larger than those of the $A - X$ transition. The transition moment curve of the $E - X$ transition shows a maximum around $4.0 a_0$, whereas for the $A - X$

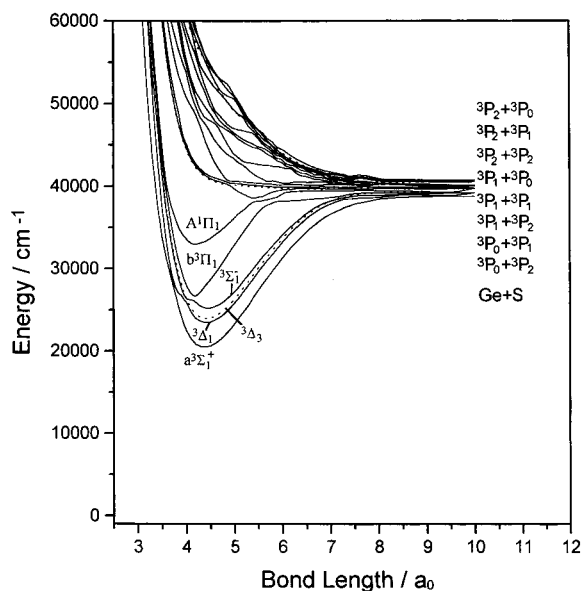


Figure 4. Potential-energy curves of low-lying 1 and 3 states of GeS (curves with dashed lines are for $\Omega = 3$).

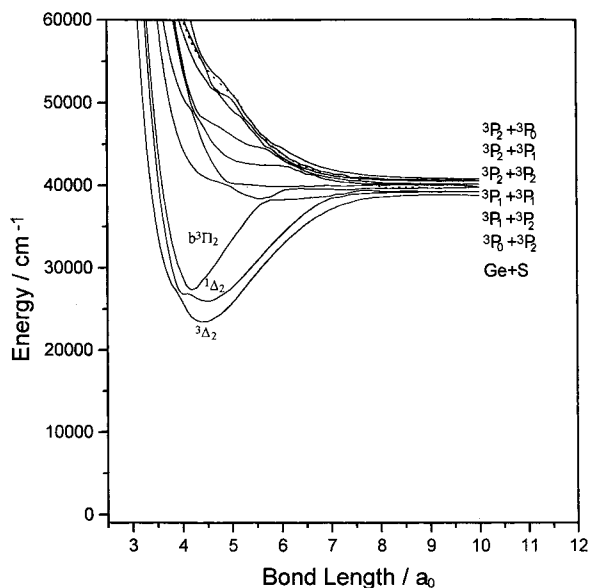


Figure 5. Potential-energy curves of low-lying 2 and 4 states of GeS (the curve with dashed line is for $\Omega = 4$).

transition, the curve is monotonically decreasing with the bond length. The radiative lifetimes of the excited $A^1\Pi$ and $E^1\Sigma^+$ states at $v' = 0$ are computed as 0.208 and 0.449 μs , respectively (see Table 5). The computed dipole moment of GeS in the ground state is about 2.54 D as compared with the observed value 2.0 ± 0.24 D.²⁸

Experimentally,¹⁹ a strong A–X absorption band of GeS in the gas phase has been found to originate at 32 889 cm^{-1} . In a low-temperature matrix, only solvent-induced phosphorescence is observed.²⁰ The phosphorescence has been assigned by Meyer et al.^{19,20} to the $a^3\Pi-X^1\Sigma^+$ transition which has been reassigned to $a^3\Sigma^+-X^1\Sigma^+$ by Linton²¹ from the chemiluminescent studies. The $b^3\Pi-X^1\Sigma^+$ Cameron band of GeS has also been observed.²¹ The lifetimes for the Cameron band of GeS in argon, krypton, and xenon at 20 and 33 K, and in SF_6 at 20, 30, and 77 K, fall in the range 625–3000 μs .²⁰

Transition probabilities of the spin-forbidden transitions in the Cameron band have been computed here. In Figure 6b,c, we have plotted the computed transition moments of 10 such

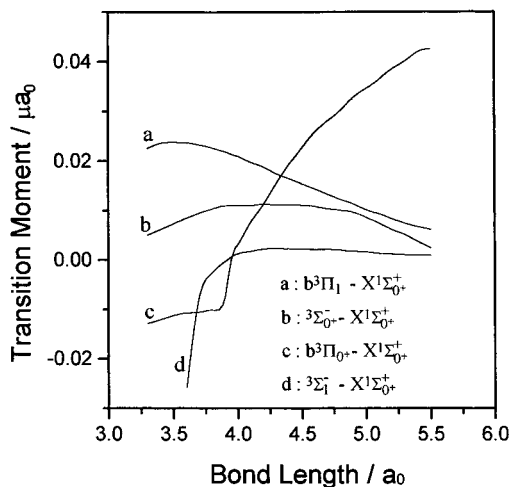
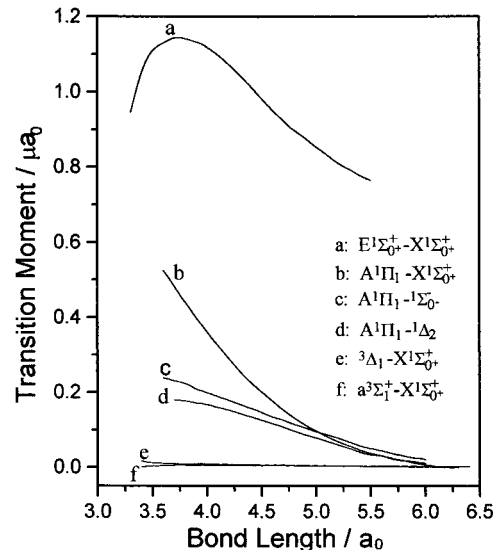
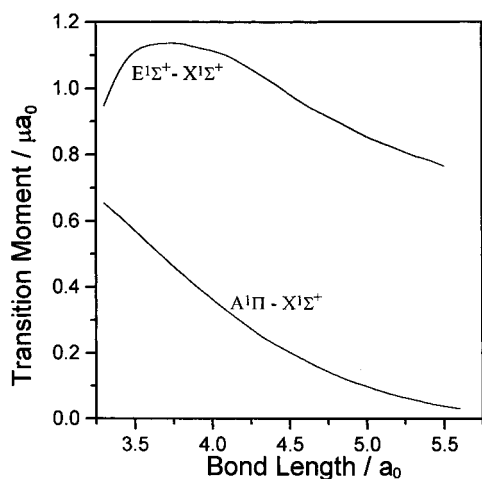


Figure 6. (a) Transition-moment functions of $A^1\Pi-X^1\Sigma^+$ and $E^1\Sigma^+-X^1\Sigma^+$ transitions of GeS. (b) Transition-moment functions of six transitions involving several spin-orbit components. (c) Transition-moment functions some other transitions.

transitions as a function of the bond length. The partial lifetimes of $A^1\Pi_1$, $^3\Delta_1$, $E^1\Sigma_0^+$, $a^3\Sigma_1^+$, $^3\Sigma_0^+$, $^3\Sigma_1^-$, $b^3\Pi_0^+$, and $b^3\Pi_1$ states at the three lowest vibrational levels are estimated. The $A^1\Pi_1-X^1\Sigma_0^+$ transition is found to be quite strong as compared with the other two transitions such as $A^1\Pi_1-^1\Sigma_0^-$ and $A^1\Pi_1-^1\Delta_2$. The computed total lifetime of the $A^1\Pi_1$ component is about 0.226 μs . The $^3\Delta_1-X^1\Sigma_0^+$ transition is, however, weak, with

TABLE 5: Radiative Lifetime(s) of Low-Lying Excited States at the Lowest Three Vibrational Levels of GeS^a

transition	lifetime of the upper state			total lifetime of upper state at $v' = 0$
	$v' = 0$	$v' = 1$	$v' = 2$	
$A^1\Pi \rightarrow X^1\Sigma^+$	2.08 (-7)	2.07 (-7)	2.05 (-7)	$\tau(A^1\Pi) = 2.08 (-7)$
$E^1\Sigma^+ \rightarrow X^1\Sigma^+$	4.49 (-7)	1.34 (-7)	0.78 (-7)	$\tau(E^1\Sigma^+) = 4.49 (-7)$
$A^1\Pi_1 \rightarrow X^1\Sigma_0^+$	2.28 (-7)	2.77 (-7)	2.67 (-7)	
$A^1\Pi_1 \rightarrow X^1\Sigma_0^-$	6.10 (-5)	5.60 (-5)	5.66 (-5)	
$A^1\Pi_1 \rightarrow ^1\Delta_2$	8.58 (-5)	8.69 (-5)	8.80 (-5)	$\tau(A^1\Pi_1) = 2.26 (-7)$
$^3\Delta_1 \rightarrow X^1\Sigma_0^+$	6.72 (-3)	2.87 (-3)	2.43 (-3)	$\tau(^3\Delta_1) = 6.72 (-3)$
$E^1\Sigma_0^+ \rightarrow X^1\Sigma_0^+$	4.66 (-7)	1.39 (-7)	0.80 (-7)	$\tau(E^1\Sigma_0^+) = 4.66 (-7)$
$a^3\Sigma_1^+ \rightarrow X^1\Sigma_0^+$	5.43 (-3)	5.25 (-3)	5.41 (-3)	$\tau(a^3\Sigma_1^+) = 5.43 (-3)$
$^3\Sigma_0^- \rightarrow X^1\Sigma_0^+$	5.52 (-4)	6.05 (-4)	6.95 (-4)	$\tau(^3\Sigma_0^-) = 5.52 (-4)$
$^3\Sigma_1^- \rightarrow X^1\Sigma_0^+$	9.05	1.44	0.47	$\tau(^3\Sigma_1^-) = 9.05$
$b^3\Pi_0^+ \rightarrow X^1\Sigma_0^+$	7.4 (-4)	4.28 (-4)	3.04 (-4)	$\tau(b^3\Pi_0^+) = 7.4 (-4)$
$b^3\Pi_1 \rightarrow X^1\Sigma_0^+$	6.83 (-5)	7.16 (-5)	7.48 (-5)	$\tau(b^3\Pi_1) = 6.83 (-5)$

^a Values in the parentheses are powers to base 10.

the radiative lifetime of $^3\Delta_1$ in the order of milliseconds. Although, the Franck–Condon overlap factor between the curves of E and X is small, the $E^1\Sigma_0^+ - X^1\Sigma_0^+$ transition is considerably strong. The lifetime of the $E^1\Sigma_0^+$ state is computed to be 0.466 μs . We have also computed transition probabilities of transitions from $a^3\Sigma_1^+$ and $^3\Sigma_{0+1}^-$ components to the ground state ($X^1\Sigma_0^+$). The $^3\Sigma_1^- - X^1\Sigma_0^+$ transition is very weak because of negligibly small transition moments throughout the potential-energy curve. The $^3\Sigma_0^-$ and $a^3\Sigma_1^+$ components have lifetimes on the order of 0.552 and 5.43 ms, respectively. The transition probabilities of the well-studied Cameron band, which correspond to $b^3\Pi_0^+ - X^1\Sigma_0^+$ and $b^3\Pi_1 - X^1\Sigma_0^+$ transitions, are calculated. The radiative lifetimes of these bands at the lowest vibrational level fall in the range of 68–740 μs . Although no gas-phase data is available, the lifetimes of the Cameron band in the rare-gas matrixes and in SF₆ at low temperatures are comparable with the calculated values. It may be noted that the lifetime of the individual spin components is generally larger than that for the pure electronic state. The radiative lifetime of the pure $A^1\Pi$ state at $v' = 0$ in the A–X transition is 0.208 μs , as compared with the partial lifetime of 0.228 μs for the $A^1\Pi$ component associated with the $A^1\Pi_1 - X^1\Sigma_0^+$ transition. The calculations show that both the $A^1\Pi_1$ and $X^1\Sigma_0^+$ components have a very small contribution from the $b^3\Pi$ Λ -S state, which does not allow the transition to occur. As a result, the intensity of the A–X transition is reduced to a small extent. A similar situation arises in the case of the $E^1\Sigma_0^+ - X^1\Sigma_0^+$ transition for which the radiative lifetime of $E^1\Sigma_0^+$ is also slightly longer than that of the pure $E^1\Sigma^+$ state.

IV. Summary

The MRDCI calculations based on RECPs confirm that the ground state of GeS is of the $X^1\Sigma^+$ symmetry. Transition energies of four observed states, $a^3\Sigma^+$, $b^3\Pi$, $A^1\Pi$, and $E^1\Sigma^+$, agree well with the calculated values. The computed bond length of the ground state of GeS is about 0.027 Å longer than the observed r_e . However, the calculated ω_e value of the $E^1\Sigma^+$ state is much smaller than the experimentally determined value. Three states, such as $^3\Sigma^-$, $^1\Sigma^-$, and $^1\Delta$, are nearly degenerate around 25 000 cm^{-1} . Potential-energy curves of these states are very similar. The ground state is described by two important configurations: $\dots\sigma^2\pi^4$ ($c^2 = 0.67$) and $\dots\sigma^2\pi^3\pi^*$ ($c^2 = 0.22$). The experimentally known a, b, A, and E states are identified in the present calculations. The spin–orbit interactions do not

change the spectroscopic parameters much. Several sharp avoided crossings are noted in the potential-energy curves of the Ω states. The present calculations predict that both $A^1\Pi - X^1\Sigma^+$ and $E^1\Sigma^+ - X^1\Sigma^+$ transitions are considerably strong. The CI-estimated radiative lifetimes of $A^1\Pi$ and $E^1\Sigma^+$ are 0.208 and 0.449 μs , respectively. The $a^3\Sigma_1^+ - X^1\Sigma_0^+$ transition is not very strong. The radiative lifetime of the $a^3\Sigma_1^+$ component is only 5.43 ms. The $b^3\Pi_0^+ - X^1\Sigma_0^+$ and $b^3\Pi_1 - X^1\Sigma_0^+$ transitions correspond to the Cameron band of the isoivalent CO. The computed radiative lifetimes of these components of $b^3\Pi$ agree well with the experimental values. The $A^1\Pi_1$ state undergoes several transitions of which $A^1\Pi_1 - X^1\Sigma_0^+$ is the strongest one. Two other transitions, $A^1\Pi_1 - ^1\Sigma_0^-$ and $A^1\Pi_1 - ^1\Delta_2$ are also found to be strong. The total lifetime of the $A^1\Pi_1$ state at $v' = 0$ is estimated to be 0.226 μs .

Acknowledgment. The authors are grateful to Prof. Dr. Robert J. Buenker, Wuppertal, Germany, for his kind permission to use the MRDCI codes.

References and Notes

- Barrow, R. F.; Jevons, W. *Proc. Phys. Soc.* **1940**, *52*, 534.
- Barrow, R. F. *Proc. Phys. Soc.* **1941**, *53*, 116.
- Drummond, G.; Barrow, R. F. *Proc. Phys. Soc.* **1952**, *65*, 277.
- Vago, E. E.; Barrow, R. F. *Proc. Phys. Soc.* **1946**, *58*, 538.
- Elander, N.; Lagerqvist, A. *Phys. Scr.* **1971**, *3*, 267.
- Barrow, R. F.; Stone, T. J. *J. Phys. B: At. Mol. Phys.* **1975**, *8*, L13.
- Lakshminarayan, G.; Shetty, B. J.; Gopal, S. *J. Mol. Spectrosc.* **1985**, *112*, 1.
- Lakshminarayan, G.; Shetty, B. J. *J. Mol. Spectrosc.* **1988**, *130*, 155.
- Sunanda, K.; Gopal, S.; Shetty, B. J.; Lakshminarayan, G. *J. Quant. Spectrosc. Radiat. Transfer* **1989**, *42*, 631.
- Shapiro, C. V.; Gibbs, R. C.; Laubergayer, A. W. *Phys. Rev.* **1932**, *40*, 354.
- Steida, W. U.; Tiemann, E.; Törring, T.; Hoefl, J. *Z. Naturforsch.* **1976**, *31*, 374.
- Magat, P.; Le Floch, A. C.; Lebreton, J. *J. Phys. B: At. Mol. Phys.* **1980**, *13*, 4143.
- Coppens, P.; Smoes, S.; Drouart, J. *Trans. Faraday Soc.* **1967**, *63*, 2140.
- Marino, C. P.; Guerin, J. D.; Nixon, E. R. *J. Mol. Spectrosc.* **1974**, *51*, 160.
- Hoefl, J.; Lovas, F. J.; Tiemann, E.; Törring, T. *J. Chem. Phys.* **1970**, *53*, 2736.
- Hoefl, J.; Lovas, F. J.; Tiemann, E.; Törring, T. *Z. Naturforsch.* **1970**, *25 A*, 539.
- Hoefl, J.; Lovas, F. J.; Tiemann, E.; Tischer, R.; Törring, T. *Z. Naturforsch.* **1969**, *24 A*, 1217.
- Huber, K. P.; Herzberg, G. *Constants of Diatomic Molecules. Molecular Spectra and Molecular Structure*; Van Nostrand Reinhold: Princeton, 1979; Vol 4.
- Meyer, B.; Jones, Y.; Smith, J. J.; Sptizer, K. *J. Mol. Spectrosc.* **1971**, *37*, 100.
- Meyer, B.; Smith, J. J.; Spitzer, K. *J. Chem. Phys.* **1970**, *53*, 3616.
- Linton, C. *J. Mol. Spectrosc.* **1980**, *79*, 90.
- Capelle, G. A.; Brom, J. M., Jr. *J. Chem. Phys.* **1975**, *63*, 5168.
- Balfour, W. J.; Shetty, B. J. *Can. J. Chem.* **1993**, *71*, 1622.
- Uehara, H.; Horiai, K.; Sueoka, K.; Nakagawa, K. *Chem. Phys. Lett.* **1989**, *160*, 149.
- Hassanzadeh, P.; Andrews, L. *J. Phys. Chem.* **1992**, *96*, 6181.
- Köppe, R.; Schnöckel, H. *J. Mol. Struct.* **1990**, *238*, 429.
- Leszczyński, J.; Kwiatkowski, J. S. *J. Phys. Chem.* **1993**, *97*, 12189.
- Ogilvie, J. F. *Mol. Phys.* **1996**, *88*, 1055.
- Manna, B.; Das, K. K. *J. Phys. Chem.* **1998**, *A 102*, 214.
- Dutta, A.; Manna, B.; Das, K. K. *Ind. J. Chem.* **2000**, *39 A*, 163.
- Hurley, M. M.; Pacios, L. F.; Christiansen, P. A.; Ross, R. B.; Ermler, W. C. *J. Chem. Phys.* **1986**, *84*, 6840.
- Pacios, L. F.; Christiansen, P. A. *J. Chem. Phys.* **1985**, *82*, 2664.
- Buenker, R. J.; Peyerimhoff, S. D. *Theor. Chim. Acta* **1974**, *35*, 33.
- Buenker, R. J.; Peyerimhoff, S. D. *Theor. Chim. Acta* **1975**, *39*, 217.

- (35) Buenker, R. J. *Int. J. Quan. Chem.* **1986**, 29, 435.
- (36) Buenker, R. J. In *Proceedings of the Workshop on Quantum Chemistry and Molecular Physics*; Burton, P., Ed.; University Wollongong: Wollongong, Australia, 1980. Current Aspects of Quantum Chemistry. *Studies in Physical and Theoretical Chemistry*; Carbó, R., Ed.; Elsevier: Amsterdam, The Netherlands, 1981; Vol. 21.
- (37) Buenker, R. J.; Phillips, R. A. *THEOCHEM* **1985**, 123, 291.
- (38) Davidson, E. R. In *the World of Quantum Chemistry*; Daudel, R., Pullman, B., Ed.; Reidel: Dordrecht, The Netherlands, 1974.
- (39) Hirsch, G.; Bruna, P. J.; Peyerimhoff, S. D.; Buenker, R. J. *Chem. Phys. Lett.* **1977**, 52, 442.
- (40) Cooley, J. W. *Math. Comput.* **1961**, 15, 363.
- (41) Moore, C. E. *Atomic Energy Levels*; National Bureau of Standards: Washington, DC, 1971; Vol. 3.
- (42) Bruna, P. J.; Peyerimhoff, S. D. In *Advances in Chemical Physics*; Lawley, K. P., Ed.; Wiley: New York, 1987; Vol 67, p 1.